Automated Selection of Optimal Gaussian Fits to Arbitrary Functions in Electronic Structure Theory

CLAUDINE C. TAZARTES,[1] CHRISTOPHER R. ANDERSON,[1] EMILY A. CARTER[2]

[1]*Department of Mathematics, University of California, Los Angeles, California 90095-1555*
[2]*Department of Chemistry and Biochemistry, University of California, Los Angeles, California, 90095-1569*

Received 13 November 1997; accepted 26 March 1998

ABSTRACT: We present a method of fitting arbitrary functions to linear combinations of Gaussians. In particular, we discuss an adaptation of Prony's method, or separation of exponentials, which allows us to automatically select appropriate exponents for these Gaussians. We then apply this technique to the selection of dealiasing sets for pseudospectral electron correlation methods. We show that it can successfully choose functions that generally improve the accuracy of pseudospectral correlation energies while reducing the size of the dealiasing set chosen. © 1998 John Wiley & Sons, Inc. J Comput Chem 19: 1300–1314, 1998

Keywords: Gaussian fits; Prony's method; pseudospectral methods; electron correlation; aliasing error

Introduction

In theoretrical chemistry and physics, one frequently encounters problems in which one wishes to fit functions to linear combinations of Gaussians (e.g., dealiasing functions in pseudospectral methods,[1] fitting of the density in density functional theory (DFT) methods,[2,3] fitting products of basis functions to auxiliary basis sets,[4] fitting of pseudopotentials[5–7]). However, determining appropriate exponents for these Gaussians can be difficult.

The idea pursued in this article consists of designing automatic procedures to select such exponents. Our technique is based on Prony's method, or the separation of exponentials; although this method is designed to fit functions to decaying exponentials, a change of variables allows us to instead do the fitting to Gaussians. We first describe this method in general terms and then show

Correspondence to: E. A. Carter; e-mail: eac@chem.ucla.edu
Contract/grant sponsor: Office of Naval Research

CCC 0192-8651 / 98 / 111300-15

how it can be used in a specific application: finding dealiasing functions in pseudospectral electron correlation methods.

Work by Friesner[8] suggested that basis function representations of the one-electron wave functions ψ may be combined with grid-based representations (the ''pseudospectral'' method). On a grid, the Coulomb operator can be represented as a sparse matrix; to apply the Coulomb operator, we transform the wave function ψ to a grid (physical) space representation, apply the operator on the grid, and then transform back to ''spectral'' (coefficient) space. This approach reduces the scaling of the two-electron integral calculations from K^4 to roughly K^3, where K is the number of basis functions.

The transformation from physical into spectral space produces components outside the original basis set, the so-called aliasing terms.[9–11] The strategy proposed by Friesner to reduce aliasing effects is to add a number of ''dealiasing'' functions to the original basis set; the role of these dealiasing functions is to complement the basis set in accurately ''capturing'' the behavior of the functions occurring in the calculation to make their transformations more accurate. However, it is not clear how best to choose these dealiasing functions.

In this work, we discuss the development of a systematic means of choosing appropriate dealiasing sets and numerical approximations to the relevant integrals; the idea is that an adequate representation of the components outside the span of the original basis set will minimize the error incurred in the transformation between grid and basis function representations. We choose suitable dealiasing sets by studying the grid-based quantities that are to be transformed back into spectral space and by fitting them to atom-centered, Cartesian Gaussians via a method called separation of exponentials. The Gaussians resulting from the fit (or, rather, some average or subset of them) are used as our dealiasing sets.

In addition to the development of the mechanism for picking dealiasing functions, we explore the application of this technique to electron correlation calculations for several molecules. These computations not only illustrate the usefulness of our method by their favorable comparison to previously published results, but also are crucial in guiding the development of a general mathematical procedure that can be used for other applications.

Fitting a Function to Gaussians

The general nature of the approximation problem is as follows: Suppose that we have a real-valued function $y(\rho, \theta, \phi)$. We would like to fit y to a linear combination of Gaussians. If $y(\rho, \theta, \phi)$ has a strong radial dependence and a weak (θ, ϕ) dependence, then it is reasonable to consider fitting y to functions of the form

$$y = \sum_{i=1}^{m} A_i e^{-\lambda_i \rho^2}.$$

Of course, this (θ, ϕ) dependence may not be known *a priori*, but it may be ascertained through computational tests, as was done in ref. 11.

SEPARATION OF EXPONENTIALS

The challenge is to select appropriate coefficients A_i and exponents λ_i. This is a problem of spectral estimation, and a variety of methods exist[12] for fitting discrete data to linear combinations of exponentials $e^{-\lambda x}$. (We will discuss the adjustment needed to fit to Gaussians $e^{-\lambda x^2}$ in a later section.)

One particularly suitable technique for fitting equally spaced data points to damped exponentials is Prony's method.[12] Prony's method is known to be sensitive to noise, but because our discrete data are determined by numerical evaluations of functions, the noise level is negligible, and Prony's method works satisfactorily.

The idea behind Prony's method is as follows: if a (discretized) function $y(x)$ looks like

$$y(x_i) = A_1 e^{-\lambda_1 x_i} + A_2 e^{-\lambda_2 x_i} + \cdots + A_m e^{-\lambda_m x_i}, \quad (1)$$

then, just as linear sums of exponentials satisfy constant-coefficient linear differential equations, y satisfies a linear, constant-coefficient difference equation, and the λ_i are identified from solutions of the difference equation

$$c_0 y(x) + c_1 y(x + h) + \cdots + c_m y(x + mh) = 0. \quad (2)$$

Specifically, suppose that we are given a set of $2m$ data points (x_i, y_i), $y_i = y(x_i)$, where the x_i

are equispaced by h:

$$x_i = x_1 + h*(i-1).$$

We want our y_i values to satisfy eq. (2), and taking $c_m = 1$, we can generate a system of linear equations for the remaining c_i:

$$\begin{aligned} c_0 y_1 + c_1 y_2 + \cdots + c_{m-1} y_m &= -y_{m+1}, \\ c_0 y_2 + c_1 y_3 + \cdots + c_{m-1} y_{m+1} &= -y_{m+2}, \\ &\vdots \\ c_0 y_m + c_1 y_{m+1} + \cdots + c_{m-1} y_{2m-1} &= -y_{2m}. \end{aligned}$$

We now have an $m \times m$ matrix equation for the coefficients,

$$\mathbf{Yc} = -\mathbf{y}, \tag{3}$$

where $\mathbf{Y}$ is the $m \times m$ matrix of y_i values such that $\mathbf{Y}(i, j) = y_{i+j-1}$; $\mathbf{c}$ and $\mathbf{y}$ are vectors of length m, where $\mathbf{c}(i) = c_i$ and $\mathbf{y}(i) = y_{i+m}$. Thus, we obtain $\mathbf{c}$ by solving the matrix equation given in eq. (3).

Once we have the c_i, we can construct solutions to the difference equation, eq. (2), by assuming solutions of the form of eq. (1), that is,

$$\begin{aligned} c_0\left(\sum_{j=1}^{m} A_j e^{-\lambda_j x}\right) + c_1\left(\sum_{j=1}^{m} A_j e^{-\lambda_j (x+h)}\right) + \cdots \\ + c_m\left(\sum_{j=1}^{m} A_j e^{-\lambda_j (x+mh)}\right) = 0, \\ \Rightarrow A_1 e^{-\lambda_1 x}\left(\sum_{k=0}^{m} c_k e^{-\lambda_1 kh}\right) \\ + A_2 e^{-\lambda_2 x}\left(\sum_{k=0}^{m} c_k e^{-\lambda_2 kh}\right) + \cdots \\ + A_m e^{-\lambda_m x}\left(\sum_{k=0}^{m} c_k e^{-\lambda_m kh}\right) = 0. \end{aligned}$$

This yields an mth degree polynomial equation,

$$c_0 + c_1 \xi + c_2 \xi^2 + \cdots + c_m \xi^m = 0, \tag{4}$$

where

$$\xi_j = e^{-\lambda_j h}$$

and $\xi_1, \xi_2, \ldots, \xi_m$ are the m roots of eq. (4). These roots can be found using standard eigenvalue methods.[13] These methods make use of the fact that the eigenvalues of an $m \times m$ matrix $\mathbf{A}$ are the roots of the characteristic polynomial

$$P(x) = \det(\mathbf{A} - \xi \mathbf{I}),$$

where $\mathbf{I}$ is the $m \times m$ identity matrix and det denotes a determinant.

Thus, to find the roots of the polynomial given in eq. (4), we use the fact that the characteristic polynomial of the $m \times m$ companion matrix,

$$\mathbf{A} = \begin{bmatrix} \frac{-c_{m-1}}{c_m} & \frac{-c_{m-2}}{c_m} & \cdots & \frac{-c_1}{c_m} & \frac{-c_0}{c_m} \\ 1 & 0 & \cdots & 0 & 0 \\ 0 & 1 & \cdots & 0 & 0 \\ \cdot & \cdot & \cdot & \cdot & \cdot \\ \cdot & \cdot & \cdot & \cdot & \cdot \\ 0 & 0 & \cdots & 0 & 1 \end{bmatrix},$$

is equivalent to eq. (4). Thus, by finding the eigenvalues of $\mathbf{A}$, we are finding the roots of eq. (4).

Once we have the ξ_j, we can find the exponents λ_j trivially from

$$\lambda_j = -\frac{1}{h}\ln(\xi_j).$$

If we also want to determine the coefficients A_i, we can generate a linear system of equations for them by requiring that the y_i be of the form of eq. (1):

$$\begin{aligned} A_1 e^{-\lambda_1 x_1} + A_2 e^{-\lambda_2 x_1} + \cdots + A_m e^{-\lambda_m x_1} &= y_1, \\ A_1 e^{-\lambda_1 x_2} + A_2 e^{-\lambda_2 x_2} + \cdots + A_m e^{-\lambda_m x_2} &= y_2, \\ &\vdots \\ A_1 e^{-\lambda_1 x_{2m}} + A_2 e^{-\lambda_2 x_{2m}} + \cdots + A_m e^{-\lambda_m x_{2m}} &= y_{2m}. \end{aligned}$$

Note that this is an overdetermined system,

$$\mathbf{EA} = \mathbf{y}, \tag{5}$$

where $\mathbf{E}$ is the $2m \times m$ matrix described by $\mathbf{E}(i, j) = e^{-\lambda_i x_j}$, $\mathbf{A}$ is the vector of length m such that $\mathbf{A}(i) = A_i$, and $\mathbf{y}$ is the vector of length $2m$ such that $y(i) = y_i$. We can solve this system in the least squares sense either by directly using a singular value decomposition on the overdetermined system or by solving the ''normal'' equations (using, e.g., Gaussian elimination with pivoting):

$$\mathbf{E}^T \mathbf{EA} = \mathbf{E}^T \mathbf{y}.$$

REDUCING SYSTEM SIZE

In order to reduce the system size (and hence reduce the order of the polynomial whose roots we must find), we use the technique proposed by Lanczos.[14] We do not use consecutive values of y_i

in eq. (3). Instead, we divide the data into groups and use the sum of the ordinates in each group as our y_i. For example, suppose that we have 60 data points and we want to use $m = 5$ exponentials in our fitting procedure. We can separate these into $2m = 10$ groups of 6 values each. The sum of the 6 values in each of these 10 groups gives us 10 new values, $\tilde{y}_i$, which we can use in eq. (3).

For our data sets, the linear system (3) is not very large and we solve the system using Gaussian elimination (with pivoting). For larger systems, the special structure of $\mathbf{Y}$ (with rearrangement of the rows, it is a Toeplitz matrix[15]) can be exploited and more efficient solvers are available.[13,15]

FITTING TO GAUSSIANS

Our task is to find functions of the form

$$y_i = \sum_{j=1}^{m} A_j e^{-\lambda_j x_i^2},$$

which are Gaussians instead of damped exponentials. To apply the technique described above, we simply fit exponentials to the data (t_i, y_i), where the t_i are equispaced and

$$y_i = y(x_i),$$
$$t_i = x_i^2.$$

Thus,

$$y_i = \sum_{j=1}^{m} A_j e^{-\lambda_j t_i} = \sum_{j=1}^{m} A_j e^{-\lambda_j x_i^2},$$

as required.

Application: Dealiasing in Pseudospectral Electron Correlation Methods

We used the fitting procedure described above to systematically select dealiasing functions[9] in pseudospectral electron correlation methods. A computational component of these methods is to numerically evaluate the two-electron integrals:

$$(ij|kl) = \langle \phi_i | \mathscr{J}^{kl} | \phi_j \rangle = \int_{\mathbb{R}^3} \int_{\mathbb{R}^3} \frac{\phi_i(\mathbf{r}) \phi_j(\mathbf{r}) \phi_k(\mathbf{r}') \phi_l(\mathbf{r}')}{|\mathbf{r} - \mathbf{r}'|} \, d\mathbf{r} \, d\mathbf{r}', \quad (6)$$

$$\mathscr{J}^{kl}(\mathbf{r}) = \int_{\mathbb{R}^3} \frac{\phi_k(\mathbf{r}') \phi_l(\mathbf{r}')}{|\mathbf{r} - \mathbf{r}'|} \, d\mathbf{r}'.$$

We will first describe the pseudospectral approximation to two-electron integrals and how this approximation leads to aliasing errors. We will then discuss how to select dealiasing functions, the purpose of which is to reduce aliasing effects. We will limit our discussion to treatment of the Coulomb operator $\mathscr{J}^{kl}$; the exchange operator can be treated similarly.

TWO REPRESENTATIONS OF ψ

In pseudospectral methods, we make use of two different representations of the one-electron orbital ψ. One of them is a basis function representation,

$$\psi = \sum_{n=1}^{K} c_n \phi_n, \quad (7)$$

where the ϕ_n are a set of known basis functions. We take them to be normalized, atom-centered Cartesian Gaussians.

The other representation we use is a physical, or grid-based representation, first proposed by Friesner;[8] thus, we introduce a set of G grid points,

$$\mathbf{r}_1, \mathbf{r}_2, \ldots, \mathbf{r}_G \in \mathbb{R}^3,$$

and a $G \times K$ collocation matrix $\mathbf{R}$ of basis functions ϕ_n evaluated at these grid points; that is,

$$\mathbf{R}(g, n) = \phi_n(\mathbf{r}_g). \quad (8)$$

Then the grid-based version of ψ can be written as

$$\psi = \begin{bmatrix} \psi(\mathbf{r}_1) \\ \psi(\mathbf{r}_2) \\ \cdot \\ \cdot \\ \cdot \\ \psi(\mathbf{r}_G) \end{bmatrix}$$

or

$$\boldsymbol{\psi} = \mathbf{R}\mathbf{c}, \quad (9)$$

where $\mathbf{c}$ is a vector of coefficients $c_1, \ldots, c_K$.

PSEUDOSPECTRAL TWO-ELECTRON INTEGRALS AND NEED FOR DEALIASING

The two-electron integral $(ij|kl) \equiv \langle \phi_i | \mathscr{J}^{kl} | \phi_j \rangle$ may be thought of as a projection of the function $\phi_j \mathscr{J}^{kl}$ onto the basis set $\{\phi_n\}_{n=1}^{K}$. This means that

the function $\phi_j(\mathbf{r})\mathscr{J}^{kl}(\mathbf{r})$ can be expressed as a linear combination of the ϕ_n, with some coefficients P_{nj}^{kl}, so that the $(ij|kl)$ may be written as follows:

$$\begin{aligned}\phi_j(\mathbf{r})\mathscr{J}^{kl}(\mathbf{r}) &= \sum_{n=1}^{K} P_{nj}^{kl}\phi_n(\mathbf{r}),\\ \Rightarrow (ij|kl) \equiv \langle \phi_i|\mathscr{J}^{kl}|\phi_j\rangle &= \sum_{n=1}^{K} P_{nj}^{kl}\langle \phi_i \mid \phi_n\rangle.\end{aligned} \tag{10}$$

We would like to use pseudospectral approximations to the two-electron integrals $(ij|kl)$. Thus, we define an inner product, $\langle \cdot \mid \cdot \rangle_w$, with associated weights w_g, $g = 1, \ldots, G$:

$$\langle f \mid y\rangle_w = \sum_{g=1}^{G} f(\mathbf{r}_g)\, y(\mathbf{r}_g) w_g.$$

Pseudospectral approximations to the $(ij|kl)$ are obtained by replacing one of the analytical integrations over $\mathbb{R}^3$ in $(ij|kl)$ [see eq. (7)] with a numerical approximation:

$$\begin{aligned}(ij|kl) &\simeq \langle \phi_i|\mathscr{J}^{kl}|\phi_j\rangle_w\\ &= \sum_{g=1}^{G} \phi_i(\mathbf{r}_g)\phi_j(\mathbf{r}_g) w_g \int_{\mathbb{R}^3} \frac{\phi_k(\mathbf{r})\phi_l(\mathbf{r})}{|\mathbf{r}-\mathbf{r}_g|}\, d\mathbf{r}.\end{aligned} \tag{11}$$

We introduce the following notation,

$$f_{j,k,l} \equiv \phi_j \mathscr{J}^{kl}.$$

Thus, we can write

$$(ij|kl) = \langle \phi_i \mid f_{j,k,l}\rangle \simeq \langle \phi_i \mid f_{j,k,l}\rangle_w.$$

The success of the pseudospectral method depends on our ability to compute numerical inner products accurately. The $f_{j,k,l}$ are projected onto the space spanned by the ϕ_n, but they may contain components not in this space that can contaminate the $\langle \phi_i \mid f_{j,k,l}\rangle_w$. These are called aliasing terms.

To illustrate that there is indeed an accuracy problem, we show pseudospectral second-order Møller–Plesset perturbation theory (MP2) calculations[16] in Table I for acetylene on three different grid sizes (coarse, medium, and fine PSGVB v1.00 grids[17]). E_s is the spectral MP2 correlation energy (i.e., all integrals are calculated analytically), and E_{ps} is the MP2 correlation energy calculated using numerical approximations.

We point out here that these results were obtained using straight numerical quadrature [as seen in eq. (11)], as opposed to the more accurate approach used by Martinez and Carter.[16] See Appendix A for more details.

TABLE I.
Simple Numerical Quadrature[a] MP2 Calculations on Different Grid Sizes for C_2H_2.

6–31G** Basis Sets for C_2H_2 ($K = 40$); E_s[b] $= -0.267687$ hartrees

Grid	No. Grid Points	E_{ps}[c] (hartrees)	$\lvert E_s - E_{ps}\rvert$[d] (hartrees)
Coarse	296	−0.258145	9.452e-03
Medium	754	−0.272333	4.646e-03
Fine	3952	−0.267100	5.87e-04

[a] See eq. (11) and Appendix A.
[b] Spectral MP2 correlation energy.
[c] Pseudospectral MP2 correlation energy.
[d] Difference (in absolute value) between spectral and pseudospectral MP2 correlation energies.

We see that as we refine the grid, the pseudospectral correlation energies become more accurate; to get to within 1 mhartree of the spectral results, we need to use fine grids where $G > K^2$. However, the pseudospectral approximation is advantageous only if $G < K^2$.[8]

Thus, we must make adjustments to our numerical approximations so that we obtain sufficient accuracy in the inner products without using such fine grids.

DEALIASING FUNCTIONS

To address the problems with our inner product rule, let us consider the physical space projection of $f_{j,k,l} \equiv \phi_j \mathscr{J}^{kl}$ onto $\{\phi_n\}_{n=1}^K$:

$$\begin{aligned}f_{j,k,l}(\mathbf{r}_g) &= \sum_{n=1}^{K} P_{nj}^{kl}\phi_n(\mathbf{r}_g),\\ \Rightarrow \langle \phi_i \mid f_{j,k,l}\rangle_w &= \sum_{n=1}^{K} P_{nj}^{kl}\langle \phi_i \mid \phi_n\rangle_w.\end{aligned}$$

To obtain accuracy in the $\langle \phi_i \mid f_{j,k,l}\rangle$ we need to ensure the accuracy of the $\langle \phi_i \mid \phi_n\rangle_w$, but we also need to ensure that $\langle \cdot \mid \cdot \rangle_w$ is accurate for components of $f_{j,k,l}$ outside the span of $\{\phi_n\}_{n=1}^K$.

Suppose, then, that we have functions δ_b such that

$$f_{j,k,l} \in \operatorname{span}\left(\{\phi_n\}_{n=1}^K, \{\delta_b\}_{b=1}^L\right).$$

Then[18]

$$\langle \phi_i \mid f_{j,k,l} \rangle_w = \sum_{n=1}^{K} P_{nj}^{kl} \langle \phi_i \mid \phi_n \rangle_w + \sum_{b=1}^{L} D_{bj}^{kl} \langle \phi_i \mid \delta_b \rangle_w .$$

If $\langle \phi_i \mid \phi_n \rangle_w$ and $\langle \phi_i \mid \delta_b \rangle_w$ are accurate to within some acceptable tolerance, then $\langle \phi_i \mid f_{j,k,l} \rangle_w$ will also be sufficiently accurate.

Thus, our task is twofold: we need to find functions δ_b (called *dealiasing functiions*) that will complement our original basis functions ϕ_n by properly capturing the behavior of the $f_{j,k,l}$.

Then, once we have the δ_b, we must minimize the errors made in computing $\langle \phi_i \mid \phi_n \rangle_w$ and $\langle \phi_i \mid \delta_b \rangle_w$; to do so, we must define and impose some constraints on $\langle \cdot \mid \cdot \rangle_w$. In the same way that specialized quadrature rules are designed to work for certain classes of functions, we will redefine our quadrature rule so that it is accurate specifically for the types of inner products we want to compute.

In this article we are concerned mainly with the selection of dealiasing functions, and we turn our attention to this problem in the next section. A description of the quadrature rule that we used for all results presented below is given in Appendix A.

Choosing Dealiasing Functions δ_b

We now discuss the technique we use to choose our dealiasing functions δ_b. As discussed in the previous section, we need to pick dealiasing functions that will supplement our original basis functions ϕ_m in properly capturing the behavior of the $f_{j,k,l}$. Thus, we need to pick our δ_b so that the $f_{j,k,l}$ can be well represented by the set of functions $\{\{\phi_m\}_{m=1}^{K}, \{\delta_b\}_{b=1}^{L}\}$. It therefore seems reasonable to fit the $f_{j,k,l}$ to a set of functions and use these as our dealiasing functions.

Ringnalda et al.[1] and Friesner[9] propose that the dealiasing functions be of the same form as the atomic orbitals ϕ_m (i.e., atom-centered normalized Cartesian Gaussians). This facilitates the computation of certain necessary inner products ($\langle \phi_m \mid \phi_n \rangle$, $\langle \phi_m \mid \delta_b \rangle$; see Appendix A); also, as we shall see shortly, in most cases the $f_{j,k,l}$ functions that we are trying to capture roughly mimic the behavior of ϕ_j in the radial direction. Thus, atom-centered normalized Cartesian Gaussians seem like a reasonable choice for the δ_b. However, we must pick exponents for these Gaussians.

To this end, we fit the $f_{j,k,l}$ to linear combinations of Gaussians using the procedure outlined in an earlier section. In this way, we can identify functions that adequately represent the $f_{j,k,l}$ and use these functions (or some subset of them) as our δ_b.

Theoretically, we fit only the radial component of the $f_{j,k,l}$. (In actuality, the $f_{j,k,l}$ are not really separable, but we found that the angular components have little effect on the overall fitting procedure.[11] In particular, in calculations on C_2H_2 and C_2H_4 that tested how the angular components affected the MP2 energy, we found variations in the optimal dealiasing exponents of up to 11%; but these resulted in variations in the MP2 energy of, in the worst case, 76 μhartree.) Also, for simplicity, we only fit the $f_{j,k,k}$, which seemed to well represent the entire set of $f_{j,k,l}$.

MODEL PROBLEM: HYDROGEN ATOM

We center our hydrogen atom and its basis functions (we use the 6–31G** sets) at the origin and choose our grid points to be of the form $\mathbf{r}_g = (0, 0, z_g)$, where the z_g are positive and their squares, t_g, are evenly spaced:

$$t_g = z_g^2, \qquad 0.08 \le z_g \le 4 \text{ bohr},$$
$$h = t_{g+1} - t_g = 0.27 \quad (G = 60).$$

We then do the fitting of the $f_{j,k,k}$. There are five functions in the basis set (two s functions, and one each of p_x, p_y, p_z), but $p_x = p_y = 0$ everywhere on our grid; thus, there are only three possible choices for j. There are four possible choices for k (because $\mathcal{I}^{kk}$ is the same for p_x and p_y), so we are fitting 12 $f_{j,k,k}$ functions.

We found that five Gaussians usually provides us with a good fit; in most cases, using fewer than five Gaussians does not give us an accurate enough fit to the $f_{j,k,k}$, and using more than five does not appreciably increase the accuracy of the fit. Moreover, using large numbers of functions increases the system size in eqs. (3) and (5) and increases the chances of generating ill-conditioned systems. However, in some instances more than five Gaussians may be needed to obtain reasonable fits to the $f_{j,k,k}$.[11] We also point out that, for a given $f_{j,k,k}$, using different numbers of Gaussians will yield different exponents.

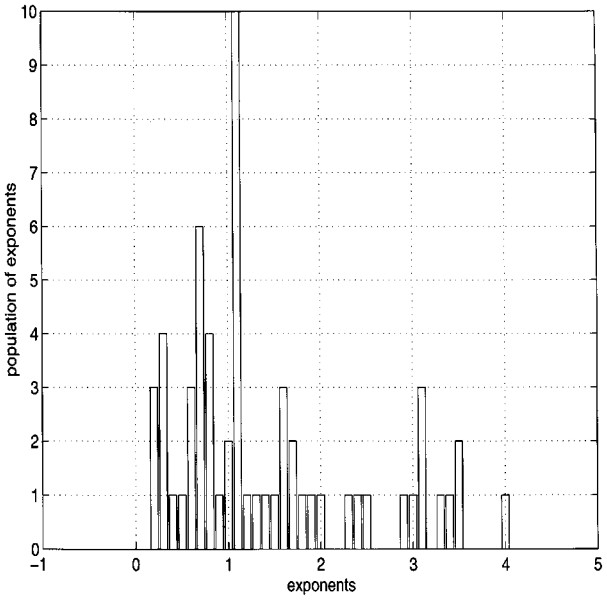

FIGURE 1. Exponents λ_i for hydrogen atom fitting.

In the case that we are currently discussing, the hydrogen atom, we fit each $f_{j,k,k}$ to five Gaussians, giving us a total of 60 exponents from which to choose (see Fig. 1). We do not want to use all of these exponents, because there are many of them and many of them are similar. Thus, we group our exponents into ''bins'' of varying widths and take averages over each of these bins to obtain exponents for our δ_b. Note that we are really only fitting to s functions (i.e., functions of the form $e^{-\lambda \mathbf{r}^2}$); however, we found it useful to also include p functions (i.e., $xe^{-\lambda \mathbf{r}^2}$, $ye^{-\lambda \mathbf{r}^2}$, $ze^{-\lambda \mathbf{r}^2}$). We found that including d-type functions does not improve our results for correlation energies of main group molecules. It is likely that such functions will be needed for transition metal containing molecules, but this is beyond the scope of the present work.

We omit from the selection process those exponents that are close to exponents already in the basis set. For example, we notice 24 values in the 0−1.0 range and ϕ_2 is an s-type function with exponent 0.167127776. Similarly, there are 22 functions in the 1.0−2.0 range and ϕ_5, a p-type basis function, has exponent 1.1. Thus, when choosing exponents for s-type δ_b functions, we will ignore the bins in the 0−1.0 range; when choosing exponents for p-type δ_b functions, we will ignore the bins in the 1.0−2.0 range.

Omitting those exponents that are in the same bin as basis functions, we use as our δ_b s functions with exponents 1.33 and 2.93 (we consider 4.12 an outlier; including it or not in our averaging made no difference) and p functions with exponents 0.56 and 2.93. Note that for larger exponents we choose larger bin widths (as the exponents get larger, the corresponding Gaussians look more and more alike; see Table II).

DEALIASING SETS FOR LARGER SYSTEMS

Now suppose that we want to find dealiasing sets for use in molecules containing more than one type of atom. Then we need to fit $f_{j,k,k}$ functions where the ''j'' function is centered at one nucleus and the ''k'' function is centered at another. In Figures 2 and 3 we show some plots of $f_{j,k,k}$ functions: a typical case and a case in which the shape of $f_{j,k,k}$ deviates noticeably from that of ϕ_j, respectively. In both cases, ϕ_j is a ''tight'' contracted s-type function (six contracted Gaussians) from the 6−31G** hydrogen set. In Figure 2 the k functions belong to the 6−31G** hydrogen set, and in Figure 3 the k functions belong to the 6−31G** carbon set. Figure 4 shows ϕ_j by itself. We can see that, in most cases, the $f_{j,k,k}$ roughly follows the behavior of ϕ_j, except in Figure 3; for $k = 1$ from the carbon basis set (contracted, tight s function), $\mathcal{J}^{kk}$ is large and has a pronounced peak near the carbon center; it would appear from these figures that this peak is not completely eliminated by the hydrogen j function.

Thus, because the $f_{j,k,k}$ *usually* look roughly like Cartesian Gaussians centered at the j function's nucleus, we fit the $f_{j,k,k}$ to get δ_b corresponding to the j basis functions.

For example, if we want δ_b for hydrogen in a molecule that also contains carbon, we use the hydrogen basis functions as our j functions and

TABLE II.
Sums of Exponents λ_i for Hydrogen Atom Fitting.

	$0 < \lambda_i < 1$	$1 \le \lambda_i < 2$	$2 \le \lambda_i < 3$	$3 \le \lambda_i < 4$	$4 \le \lambda_i$
No. Exponents	24	22	5	8	1
Sum	13.458	29.326	12.080	26.006	4.1207
Average	0.56	1.33	2.93		4.12

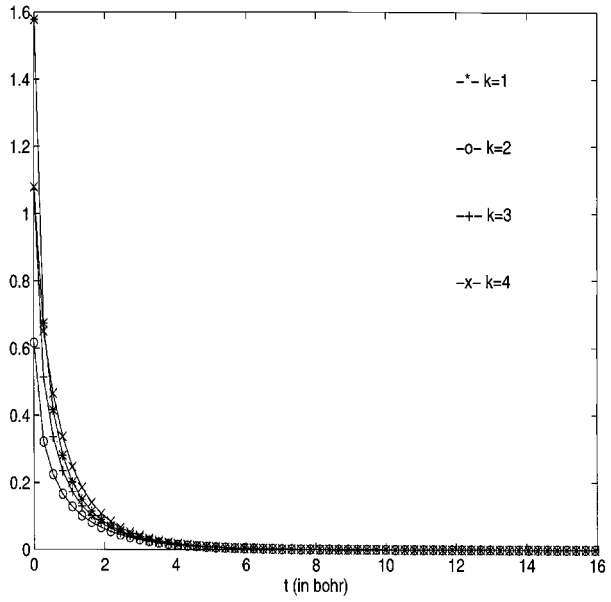

FIGURE 2. $f_{1,k,k}$: $j = 1$ on H (contracted s function); $k = 1, 2, 3$, and 5 on H.

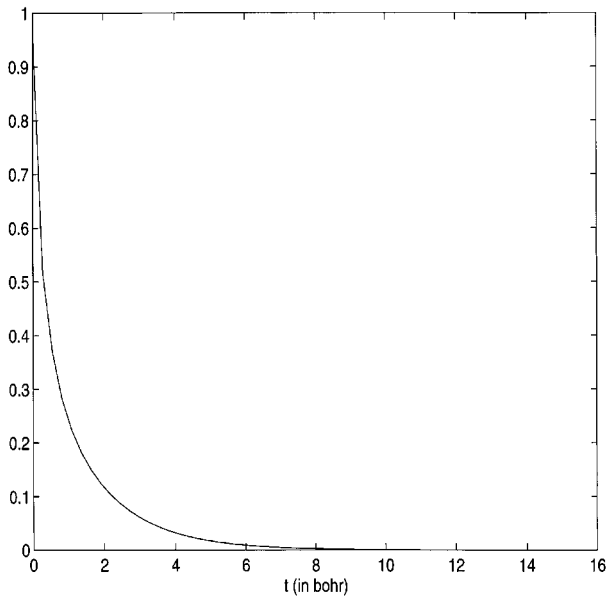

FIGURE 4. ϕ_1 for hydrogen 6–31G** set (contracted s function).

the carbon functions as our k functions. We center the hydrogen atom at $(0, 0, 0)$ and the carbon atom on the positive z axis at the desired distance from $(0, 0, 0)$. We then fit the $f_{j,k,k}$ and pool the resulting exponents together with those from the single hydrogen atom fitting. We can now average over the appropriate bins to obtain dealiasing functions for hydrogen. To get dealiasing functions for carbon, we simply reverse the roles and positions of the carbon and hydrogen atoms in the procedure above. Some dealiasing sets for different combinations of atoms are given in Appendix B.

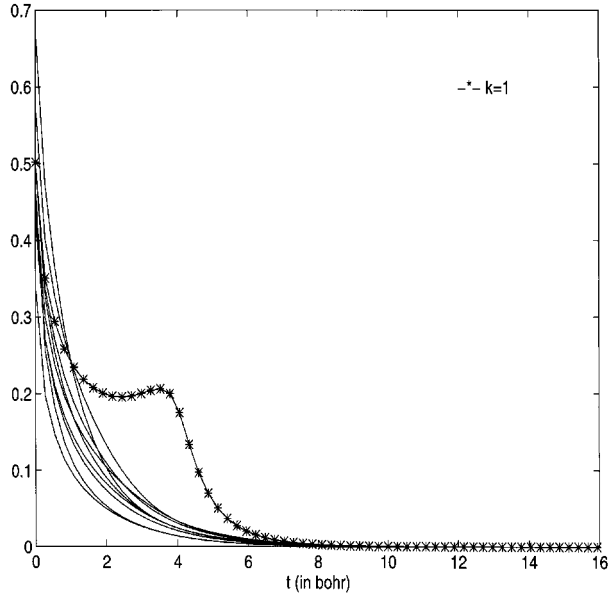

FIGURE 3. $f_{1,k,k}$: $j = 1$ on H (contracted s function); $k = 1$–3, 5–7, 9, 10, and 12–14 on C.

Note that our dealiasing sets are completely determined by the original basis sets and are not grid dependent (i.e., we do not use any information about the grids that will eventually be used in the pseudospectral calculations).

We are currently investigating how dependent the fitting process is on our choice of interatomic distances. For example, we would like to know if the fitting procedure yields the same exponents for atoms X and Y whether these atoms are, say, 1 or 2 Å apart. If the fitting procedure is not affected by distances between atoms, then we can use the procedure to compute exponents for whichever combinations of atoms we like, thereby creating a ''library'' of exponents that are available for use with any system. So, for a specific molecule, we simply extract from the library those exponents that we need, pool them together as described in the example above, and run the averaging code to obtain dealiasing functions appropriate for that molecule.

If the fitting procedure *is* affected by distances between atoms, then we can still create the exponent library described above; however, it will be more complex, because we will have exponents not only for different combinations of atoms, but also for different distances between atoms. Thus,

when we are extracting exponents from the library and pooling them together for averaging, we must make sure that we are selecting those exponents most appropriate to the distances within our molecule. For obvious reasons, this is less than desirable.

Preliminary tests indicate that interatomic distances seem to have little impact on the exponents obtained, but more tests are needed to see if this is generally true. In the first row of Table III our j functions are all hydrogen 6−31G** basis functions and our k functions are carbon and hydrogen 6−31G** basis functions; we show the average exponents when the hydrogen and carbon atoms are 1.057 Å apart and when they are 2.2398 Å (approximately twice the previous distance) apart.[19] The second row is similar, with the j functions are now on carbon and the k functions on both hydrogen and carbon. (See Table B.II in Appendix B for a few pseudospectral correlation energies comparing the δ_b functions from Table III). We see that the results from the two δ_b sets are nearly identical. This points to our δ_b sets being transferable (i.e., it does not appear that we need to run the fitting procedure for many different interatomic distances).

TABLE III.
Average Exponents for Hydrogen and Carbon δ_b for Different Interatomic Distances.

	Distance 1: 1.057 Å	Distance 2: 2.2398 Å
Hydrogen δ_b	0.58, 1.35, 2.77, 4.12	0.51, 1.27, 2.92, 4.12
Carbon δ_b	0.56, 1.41, 3.23, 8.94	0.50, 1.45, 3.11, 8.47

We also point out here that the final choice of exponents can be sensitive to our choice of ''bin'' sizes. We experimented with various schemes (e.g., omitting any exponents within a set tolerance from a basis function exponent), but the procedure outlined above worked best for our purposes.

Results

We now present pseudospectral correlation energies for two different types of calculations, MP2 and single and double excitation configuration interaction (SDCI), in Tables IV−VI using the new dealiasing function sets given in Table B.I in Appendix B. We compare our pseudospectral results to corresponding spectral calculations, as well as to previously published pseudospectral results[16] in which PSGVB v1.00 dealiasing sets were used. In all cases, we use the PSGVB v1.00 grids. The pseudospectral quantities were calculated using codes described in refs. 10 and 11.

The sets from Table B.I used in each molecule are those that best correspond to the combination of atoms in that molecule; for example, in HCN we used the hydrogen-carbon-nitrogen dealiasing set for hydrogen, the carbon-hydrogen-nitrogen dealiasing set for carbon, and the nitrogen-carbon-hydrogen set for nitrogen (see Appendix B for a nomenclature explanation). The sets sometimes look very similar (e.g., the carbon-hydrogen set does not look appreciably different from the carbon-hydrogen-nitrogen set); substitution of one set for another may lead to only slightly less accurate pseudospectral results (see Table B.III in Appendix B), but this also needs to be studied more carefully

TABLE IV.
Errors in Pseudospectral MP2 Correlation Energies (Medium Grids).

Molecule	E_s[a]	E_{ps}[b]	$\lvert E_s - E_{ps}\rvert$[c]	Previous Error[d,16]
HF	−0.184968	−0.185212	2.44e-04	8.83e-04
H_2O	−0.198155	−0.198496	3.41e-04	5.17e-04
HCN	−0.293084	−0.292959	1.25e-04	2.65e-04
C_2H_2	−0.267687	−0.267768	8.1e-05	5.88e-04
C_2H_4	−0.288011	−0.288444	4.33e-04	6.21e-04
Ethylene oxide	−0.472735	−0.472710	2.5e-05	1.936e-03
C_4H_6	−0.559657	−0.561631	1.974e-03	1.560e-03
Glycine	−0.818312	−0.820035	1.723e-03	2.136e-03

[a] Spectral MP2 correlation energy (hartrees).
[b] Pseudospectral MP2 correlation energy (hartrees) using new δ_b sets.
[c] Difference (in absolute value) between spectral and pseudospectral MP2 correlation energies (hartrees).
[d] Pseudospectral MP2 correlation energy error (hartrees) using dealiasing function sets due to Ringnalda et al.[17]

TABLE V.
Errors in Pseudospectral SDCI Total Energies (Coarse Grids).

Molecule	E_s[a]	E_{ps}[b]	$\lvert E_s - E_{ps}\rvert$[c]	Previous Error[d, 10, 11]
H_2O	−76.223114	−76.222755	3.59e-04	3.45e-04
HCN	−93.157964	−93.157737	2.27e-04	1.70e-04
C_2H_2	−77.085583	−77.085181	4.02e-04	6.28e-04
C_2H_4	−78.330503	−78.330321	1.82e-04	1.78e-04
C_2H_6	−79.558023	−79.557723	3.00e-04	5.09e-04
Ethylene oxide	−153.319117	−153.319618	5.01e-04	2.20e-04
C_4H_6	−155.448883	−155.448765	1.18e-04	9.24e-04
Glycine	−283.556231	−283.555546	6.80e-04	6.0e-05

[a]Spectral SDCI total energy (hartrees).
[b]Pseudospectral SDCI total energy (hartrees) using new δ_b sets.
[c]Difference (in absolute value) between spectral and pseudospectral SDCI total energies (hartrees).
[d]Pseudospectral SDCI total energy error (hartrees) using dealiasing function sets due to Ringnalda et al.[17]

before we can say anything conclusive about the impact of an atom's environment on our choice of δ_b. These preliminary results, like those we obtained in studying the effect of interatomic distances on the fitting procedure, seem to point to transferability of the δ_b.

The code used to do the fitting and averaging was originally written in MATLAB,[11] although we now also have a C version of this code.[11] For more information on PSGVB, see ref. 17.

The pseudospectral MP2 calculations in Table IV were done using 6−31G** basis sets on the medium grids. It is evident that, in most cases, our results are as accurate, or more accurate, than those previously obtained. Thus, this new means of choosing the δ_b does meet accuracy requirements.

Tables V and VI present pseudospectral SDCI calculations on coarse and medium grids, respectively. On coarse grids, our results are roughly the same as those previously published.[10] On medium grids, our SDCI results show better accuracy than those using the PSGVB **Q** matrix (defined in Appendix A) with dealiasing sets developed by Ringnalda et al.[17] for self-consistent field (SCF) calculations. We also notice a marked improvement over our own SDCI coarse grid results. Our δ_b sets were designed specifically for use with the 6−31G** basis sets, though the fitting procedure can be used for any other type of Gaussian basis set. In fact, we also fit the Dunning−Huzinaga $9s5p/3s2p$ sets.[19,20] However, they were not designed with any particular grid in mind. We would then hope that as grid choices improve, so should the performance of our δ_b (as exhibited in the comparison of the two sets of SDCI results).

Some advantages of using these new sets are as follows. First, in our selection method we treat the

TABLE VI.
Errors in Pseudospectral SDCI Total Energies (Medium Grids).

Molecule	E_s[a]	E_{ps}[b]	$\lvert E_s - E_{ps}\rvert$[c]	Previous Error[d]
H_2O	−76.223114	−76.223107	7e-06	1.57e-04
HCN	−93.157964	−93.157976	1.2e-05	2.5e-05
C_2H_2	−77.085583	−77.085632	4.9e-05	4.18e-04
C_2H_4	−78.330503	−78.330602	9.9e-05	6.21e-04
C_2H_6	−79.558023	−79.557917	1.06e-04	3.04e-04
Ethylene oxide	−153.319117	−153.319128	1.1e-05	4.7e-05
C_4H_6	−155.448883	−155.448866	1.7e-05	8.98e-04
Glycine	−283.556231	−283.556155	7.6e-05	9.00e-04

[a]Spectral SDCI total energy (hartrees).
[b]Pseudospectral SDCI total energy (hartrees) using new δ_b sets.
[c]Difference (in absolute value) between spectral and pseudospectral SDCI total energies (hartrees).
[d]Pseudospectral SDCI total energy error (hartrees) using dealiasing function sets due to Ringnalda et al.[17]

aliasing problem explicitly: aliasing terms appear when we project the $f_{j,k,l}$ onto the $\{\phi_m\}_{m=1}^{K}$, and we address this problem directly by using a *systematic* process to determine appropriate dealiasing functions.

Second, our sets are more compact (8–12 dealiasing functions per atom as opposed to roughly 30 dealiasing functions per atom in the PSGVB v1.00 sets) and contain only s and p functions. However, this may be due to the fact that it is much easier to numerically estimate the much smaller correlation energies than the large SCF energies that Friesner's sets were designed to reproduce. Indeed, while our sets perform well for computing correlation energies, we find that they do not always provide us with accurate SCF energies or with accurate Fock matrices for ensuing correlation energy calculations. Even when the SCF energies are acceptable (errors on the order of 1 mhartree), the resulting pseudospectral Fock matrices do not perform well in correlation energy calculations. (MP2 calculations, for instance, frequently do not converge when these Fock matrices are used.) This is akin to the observation by Martinez and Carter[10,21] that smaller grids can be used in correlation energy calculations, even though they yield very poor SCF total energies when used in SCF calculations. In the same way we can get away with smaller and less complex dealiasing sets for correlation energy calculations than for SCF calculations. Thus, we envision cheaper correlation methods by using smaller grids and dealiasing function sets than are employed for SCF calculations.

Summary

We discussed the separation of exponentials method of fitting a (discrete) function to linear combinations of decaying exponentials and showed how the method could be slightly altered instead to represent a function as a linear combination of Gaussians.

Then we discussed the application of this method to pseudospectral electron correlation energies. In particular, we wanted to compute numerical approximations to the two-electron integrals $(ij \mid kl)$. Thus, we defined the function $f_{j,k,l} \equiv \phi_j \mathscr{I}^{kl}$, so that $(ij \mid kl) \equiv \langle \phi_i \mid f_{j,k,l} \rangle$. We introduced a numerical inner product, $\langle \cdot \mid \cdot \rangle_w$, to approximate the $\langle \phi_i \mid f_{j,k,l} \rangle$ (i.e., $\langle \phi_i \mid f_{j,k,l} \rangle \simeq \langle \phi_i \mid f_{j,k,l} \rangle_w$). In computing these inner products numerically, we are projecting the $f_{j,k,l}$ onto the space spanned by the original basis set $\{\phi_n\}_{n=1}^{K}$; however, the $f_{j,k,l}$ may contain components outside the original basis set. Thus, it seems reasonable to introduce a supplementary set of functions, called dealiasing functions, to complement our basis set to adequately represent the $f_{j,k,l}$ on the grid.

We then explained that by using appropriate dealiasing functions and adjusting our quadrature rule to be accurate for the specific types of inner products we need (see Appendix A), we could substantially improve the accuracy of pseudospectral electron correlation energies.

To determine appropriate dealiasing functions, we applied the separation of exponentials technique to fitting the functions that we wish to represent: the $f_{j,k,k}(\mathbf{r}_g) = \phi_j(\mathbf{r}_g)\mathscr{I}^{kk}(\mathbf{r}_g)$. We used certain combinations of the Gaussians resulting from the fit as our dealiasing sets, adding in higher angular momentum functions for improved accuracy.

Our procedure has worked well in both MP2 and SDCI calculations. We were able to achieve results similar to, or better than, those previously obtained with the PSGVB v1.00 dealiasing sets. We also saw in the case of the SDCI calculations that the performance of our dealiasing sets improved considerably as grids were refined. Thus, we expect that as grids are improved, our dealiasing sets should produce more accurate results.

Our dealiasing sets are compact, grid independent, and produce results generally a bit more accurate than those in refs. 10 and 16; also, we explicitly and systematically address the issue of aliasing by fitting specifically those functions that we seek to represent in grid space. However, we must point out that the final choice of dealiasing function exponents can be sensitive to bin width in our averaging procedure, as well as to the environment; it may also be sensitive to internuclear distances, something that we are currently investigating. Initial results do not show much sensitivity to interatomic distances, but more testing will be required before we can conclude that this is generally true.

Separation of exponentials can potentially be applied to other methods in quantum chemistry as well. For example, in Vahtras et al.'s auxiliary basis set expansion approach,[4] they propose that products of Gaussian basis functions be expanded as linear combinations of Gaussians,

$$\phi_i(\mathbf{r})\phi_j(\mathbf{r}) = \sum_{\mu} C_{\mu}^{ij}\theta_{\mu}, \tag{12}$$

where the ϕ are basis functions and the θ are Cartesian Gaussians (not necessarily atom centered). Here, the two-electron integrals could ultimately be computed analytically by using the expansions in eq. (12), but the expansion itself could be determined using the separation of exponentials procedure. The resulting integrals could then be used, for instance, in spectral electron correlation calculations.

Another potential application is in DFT.[2,3] Here, we need to compute quantities of the form

$$\langle \phi_i, \rho^{4/3}\phi_j \rangle, \tag{13}$$

where ρ is the electron density. The electron density is often fitted to an auxiliary basis of Gaussians, which could be fit by the procedure described in this work.

Thus, we hope that in addition to improving pseudospectral electron correlation methods, the fitting procedures presented here can be used to enhance other methods in quantum chemistry, as described in the two examples above, as well as in other areas of science.

Acknowledgments

E.A.C. and C.R.A. are grateful to the Office of Naval Research for support of this work. We thank Richard Friesner for providing us with a pseudospectral Hartree–Fock code. C.C.T. thanks Todd Martinez and Gregg Reynolds for helpful discussions and Ali Sepehr for running some sensitivity tests.

Appendix A: Q Operator

Suppose that we have a set of δ_b. We must adjust $\langle \cdot \mid \cdot \rangle_w$ so that $\langle \phi_n \mid \phi_i \rangle_w$ and $\langle \phi_n \mid \delta_b \rangle_w$ are accurate:

$$\langle \phi_n \mid \phi_i \rangle_w \equiv \sum_{g=1}^{G} \phi_n(\mathbf{r}_g)\phi_i(\mathbf{r}_g)w_g = \langle \phi_n \mid \phi_i \rangle,$$

$$\langle \phi_n \mid \delta_b \rangle_w \equiv \sum_{g=1}^{G} \phi_n(\mathbf{r}_g)\delta_b(\mathbf{r}_g)w_g = \langle \phi_n \mid \delta_b \rangle.$$

In matrix form,

$$\underset{K\times G}{\mathbf{R}^T}\ \underset{G\times G}{\mathbf{w}}\ \underset{G\times(K+L)}{\tilde{\mathbf{R}}} = \underset{K\times(K+L)}{\tilde{\mathbf{S}}}, \tag{A.1}$$

where the letters underneath the matrices denote the matrix dimensions. $\tilde{\mathbf{R}}$ and $\tilde{\mathbf{S}}$ are extended versions of the collocation matrix and the overlap matrix, respectively.

$$\tilde{\mathbf{R}} = \begin{bmatrix} \phi_1(\mathbf{r}_1) & \cdots & \phi_K(\mathbf{r}_1) & \delta_1(\mathbf{r}_1) & \cdots & \delta_L(\mathbf{r}_1) \\ \vdots & \vdots & \vdots & \vdots & \vdots & \vdots \\ \phi_1(\mathbf{r}_G) & \cdots & \phi_K(\mathbf{r}_G) & \delta_1(\mathbf{r}_G) & \cdots & \delta_L(\mathbf{r}_G) \end{bmatrix},$$

$$\tilde{\mathbf{S}} = \begin{bmatrix} \langle \phi_1 \mid \phi_1 \rangle & \cdots & \langle \phi_1 \mid \phi_K \rangle & \langle \phi_1 \mid \delta_1 \rangle & \cdots & \langle \phi_1 \mid \delta_L \rangle \\ \vdots & \vdots & \vdots & \vdots & \vdots & \vdots \\ \langle \phi_K \mid \phi_1 \rangle & \cdots & \langle \phi_K \mid \phi_K \rangle & \langle \phi_K \mid \delta_1 \rangle & \cdots & \langle \phi_K \mid \delta_L \rangle \end{bmatrix}.$$

However, eq. A.1 is usually not satisfied, except perhaps in the case of very small systems. To solve this problem, Ringnalda et al.[1] and Friesner[9] introduced a new operator, $\mathbf{Q}$ to redefine the inner product:

$$\mathbf{Q} = \mathbf{P}\mathbf{S}'(\tilde{\mathbf{R}}^T\mathbf{w}\tilde{\mathbf{R}})^{-1}\tilde{\mathbf{R}}^T\mathbf{w},$$

where $\mathbf{S}'$ is the $(K + L) \times (K + L)$ overlap matrix (including all elements of the form $\langle \delta_b \mid \delta_a \rangle$) and $\mathbf{P}$ is the $K \times (K + L)$ projection matrix whose top $K \times K$ section is the $K \times K$ identity matrix and whose remaining elements are all 0. Thus, the $K \times G$ matrix $\mathbf{Q}$ is such that $\mathbf{Q}\tilde{\mathbf{R}} = \mathbf{S}$. In this way, the quadrature rule is forced to be accurate for the specific types of inner products in which we are interested.

We generate our version of $\mathbf{Q}$ by solving the following underdetermined system for $\mathbf{Q}$:

$$\underset{K\times G}{\mathbf{Q}}\underset{G\times(K+L)}{\mathbf{w}^{1/2}\tilde{\mathbf{R}}} = \underset{K\times(K+L)}{\tilde{\mathbf{S}}}.$$

We find $\mathbf{Q}$ by solving the matrix equation

$$\tilde{\mathbf{R}}^T \mathbf{w}^{1/2} \mathbf{Q}^T = \tilde{\mathbf{S}}^T, \qquad \text{(A.2)}$$

using a singular value decomposition.[13, 15]

We now use this $\mathbf{Q}$ instead of $\mathbf{R}^T\mathbf{w}^{1/2}$ in all of our numerical inner products, so the pseudospectral two-electron integrals are

$$\langle \phi_i \mid f_{j,k,l} \rangle_w = \sum_{g=1}^{G} \mathbf{Q}(i,g)\mathbf{w}(g,g)^{1/2} \mathcal{I}^{kl}(\mathbf{r}_g)\mathbf{R}(g,j). \qquad \text{(A.3)}$$

To test these different ways of defining our quadrature rules, we did a series of MP2 calculations on the PSGVB v1.00 medium grids, using a different operator $\mathbf{A}$ in each case to define our inner product rule:

$$(ij \mid kl) = \sum_{g=1}^{G} \mathbf{A}(i,g)\mathcal{I}^{kl}(\mathbf{r}_g)\mathbf{w}(g,g)^{1/2}\mathbf{R}(g,j).$$

In Table A.1, we see that when $\mathbf{A} = \mathbf{R}^T\mathbf{w}^{1/2}$ (this is what we mean by straight numerical quadrature), E_{ps} is not very accurate and our approximation to the $\langle \phi_n \mid \phi_i \rangle$ (i.e., entries of $\mathbf{S}$) is poor. By letting $\mathbf{A} = \mathbf{Q}$ as solved for in eq. (A.2) with no dealiasing functions, we improve our $\langle \phi_n \mid \phi_i \rangle_w$ but E_{ps} actually worsens. We believe that this is because the weights w_g used in straight numerical quadrature are supposed to be appropriate for a broad class of functions, whereas $\mathbf{Q}$ is designed *only* to ensure accurate overlap integrals without any regard to the projection of the $f_{j,k,l}$. However, when $\mathbf{A} = \mathbf{Q}$ with our new dealiasing function set, we obtain a very accurate result in E_{ps} and our $\langle \phi_n \mid \phi_i \rangle_w$ are also accurate. Thus, it would appear that using *both* conditions on $\mathbf{Q}$ is what helps improve results—a better fit to $\mathbf{S}$ *and* a better job of capturing the behavior of $f_{j,k,l}$ on the grid.

TABLE A.I.
E_{ps} for C_2H_2 (Medium Grids: $G = 754$, $K = 40$).

Operator $\mathbf{A}$	E_{ps}[a]	$\lvert E_s - E_{ps}\rvert$[b]	$\lVert \mathbf{S} - \mathbf{A}\mathbf{w}^{1/2}\mathbf{R} \rVert_2$[c]
$\mathbf{R}^T\mathbf{w}^{1/2}$	−0.272333	4.646e-03	6.5387e-01
$\mathbf{Q}$	−0.279024	1.1338e-02	4.90e-04
$\mathbf{Q}$, $\{\delta_b\}_{b=1}^{40}$	−0.267768	8.1e-05	7.88e-04

[a] Pseudospectral MP2 correlation energy (hartrees).
[b] Difference (in absolute value) between spectral and pseudospectral MP2 correlation energies (hartrees).
[c] For an $N \times N$ matrix $\mathbf{M}$, $\lVert \mathbf{M} \rVert_2$ is the square root of the maximum (in absolute value) eigenvalue of $\mathbf{M}^T\mathbf{M}$.

Appendix B: Dealiasing Sets for 6−31G** Basis Sets

Table B.I lists the pseudospectral 6−31G** δ_b sets for different combinations of atoms. The atom at which the δ_b are centered is listed first, and any other atoms are placed along the *positive* z axis at the desired distance from the first atom. We place them along the positive z axis because the z variable represents a radial distance, and thus we define it to always be positive. For example, the hydrogen-carbon-oxygen set are the δ_b centered on the hydrogen atom when there are hydrogen, carbon, and oxygen atoms in the molecule. Figure B.1 shows how we positioned these atoms during the fitting procedure. (Of course, this is not how they are positioned in the subsequent energy calculations.)

None of the δ_b are contracted, so we list no contraction coefficients. The distances between atoms are given in Ångströms. We chose our interatomic distances to be the same as those used by Martinez and Carter.[10, 16]

Table B.II shows pseudospectral MP2 correlation energies using δ_b sets obtained from two separate fittings, as described in an earlier section. In the first fitting, we set the distance between the hydrogen and carbon atoms to be 1.057 Å; in the second fitting, we set the distance between the hydrogen and carbon atoms to be 2.2398 Å. The resulting exponents are shown in Table III. The results in Table B.II show that the two δ_b sets yield similar MP2 energies. (Note that the errors in the third column of Table B.II are the same as those in the fourth column of Table IV.)

We note here that the exponents for a given atom's dealiasing set do vary with that atom's environment; however, in most cases, the exponents do not vary by much. For example, the carbon exponents in the Carbon set are not very different from those in the Carbon-Hydrogen set. In Table B.III we show some MP2 energies for different δ_b sets. ''Combined'' δ_b sets refer to those sets which take into account the atom's environment within the molecule—for example, the Nitrogen-Carbon-Hydrogen set. ''Single atom'' δ_b sets are those in which only a single atom is used to find δ_b exponents—for example, the Hydrogen set. Thus the errors in the third column of Table B.III are the same as those in the fourth column of Table IV.

While further testing will be needed, the results from Tables B.II and B.III do suggest the possibil-

TABLE B.I.
Dealiasing Sets for 6–31G Basis Sets.**

Atoms (Distances)	Function Type	Exponents
Hydrogen	*s*	1.33, 2.93
	p	0.56, 2.93
Hydrogen-Carbon	*s*	1.35, 2.77
(H–C = 1.057 Å)	*p*	0.58, 2.77
Hydrogen-Oxygen	*s*	1.39, 3.18
(H–O = 0.943 Å)	*p*	0.59, 3.18
Hydrogen-Fluorine	*s*	1.40, 2.89
(H–F = 0.91 Å)	*p*	0.52, 2.89
Hydrogen-Carbon-Oxygen	*s*	1.38, 3.05
(H–C = 1.057 Å,	*p*	0.59, 3.05
H–O = 0.943 Å)		
Hydrogen-Carbon-Nitrogen	*s*	1.33, 3.02
(H–C = 1.057 Å,	*p*	0.48, 3.02
H–N = 2.192 Å)		
H–C–N–O (H–O = 1.057 Å,	*s*	1.35, 3.10
H–C = 0.943 Å,	*p*	0.51, 3.10
H–N = 2.192 Å)		
Carbon	*s*	1.46, 3.16, 9.02
	p	1.46, 3.16, 9.02
Carbon-Hydrogen	*s*	1.41, 3.23, 8.94
(C–O = 1.057 Å)	*p*	1.41, 3.23, 8.94
Carbon-Hydrogen-Oxygen	*s*	1.34, 3.28, 8.70
(C–H = 1.057 Å,	*p*	1.34, 3.28, 8.70
C–O = 1.401 Å)		
Carbon-Hydrogen-Nitrogen	*s*	1.43, 3.16, 8.58
(C–O = 1.057 Å,	*p*	1.43, 3.16, 8.58
C–N = 1.133 Å)		
C–H–N–O (C–H = 1.0569 Å,	*s*	1.37, 3.23, 8.97
C–N = 1.133 Å,	*p*	1.37, 3.23, 8.97
C–O = 1.401 Å)		
Oxygen-Hydrogen	*s*	2.78, 6.23, 11.22
(O–H = 0.943 Å)	*p*	2.78, 6.23, 11.22
Oxygen-Carbon-Hydrogen	*s*	2.88, 6.12, 10.72
(O–C = 1.401 Å,	*p*	2.88, 6.12, 10.72
O–H = 0.943 Å)		
Nitrogen	*s*	1.38, 3.67, 9.14
	p	1.38, 3.67, 9.14
Nitrogen-Carbon-Hydrogen	*s*	1.37, 3.61, 10.16
(N–H = 2.192 Å,	*p*	1.37, 3.61, 10.16
N–C = 1.133 Å)		
Fluorine-Hydrogen	*s*	2.92, 7.55, 11.24
(F–H = 0.91 Å)	*p*	2.92, 7.55, 11.24

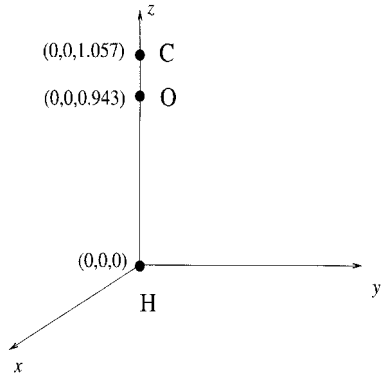

FIGURE B.1. Positions of atoms used for fitting procedure (hydrogen-carbon-oxygen δ_b set).

TABLE B.II.
Errors in Pseudospectral MP2 Correlation Energies (Medium Grids) for Different Interatomic Distance Dealiasing Sets.

Molecule	E_s[a]	$\lvert E_s - E_{ps}\rvert$[b] (Distance 1 δ_b)	$\lvert E_s - E_{ps}\rvert$[c] (Distance 2 δ_b)
C_2H_2	−0.267687	8.1e-05	9.9e-05
C_2H_4	−0.288011	4.33e-04	5.25e-04
C_4H_6	−0.559657	1.974e-03	2.067e-03

[a] Spectral MP2 correlation energy (hartrees).
[b] Difference (in absolute value) between spectral and pseudospectral MP2 correlation energies (hartrees) using Distance 1 (H–C = 1.057 Å) δ_b.
[c] Difference (in absolute value) between spectral and pseudospectral MP2 correlation energies (hartrees) using Distance 2 (H–C = 2.2398 Å) δ_b.

TABLE B.III.
Errors in Pseudospectral MP2 Correlation Energies (Medium Grids) for Different Atomic Environment Dealiasing Sets.

Molecule	E_s[a]	$\lvert E_s - E_{ps}\rvert$[b] (Combined δ_b Sets)	$\lvert E_s - E_{ps}\rvert$[c] (Single Atom δ_b Sets)
C_2H_2	−0.267687	8.1e-05	8.8e-05
C_2H_4	−0.288011	4.33e-04	4.65e-04
HCN	−0.293084	1.25e-04	1.45e-04

[a] Spectral MP2 correlation energy (hartrees).
[b] Difference (in absolute value) between spectral and pseudospectral MP2 correlation energies (hartrees) using combined δ_b sets.
[c] Difference (in absolute value) between spectral and pseudospectral MP2 correlation energies (hartrees) using single atom δ_b sets.

ity of constructing dealiasing sets which do not strongly depend on the environment of a given atom within a molecule.

References

1. M. N. Ringnalda, M. Belhadj, and R. A. Friesner, *J. Chem. Phys.* **93**, 3397 (1990).
2. B. I. Dunlap, J. W. D. Connolly, and J. R. Sabin, *J. Chem. Phys.* **71**, 3396 (1979).
3. H. Samble and R. H. Felton, *J. Chem. Phys.* **62**, 1122 (1975).
4. O. Vahtras, J. Almlöf, and M. W. Feyereisen, *Chem. Phys. Lett.* **213**, 514 (1993).
5. A. K. Rappé, T. A. Smedley, and W. A. Goddard III, *J. Phys. Chem.* **85**, 1662 (1981).
6. G. B. Bachelet, D. R. Hamann, and M. Schlüter, *Phys. Rev. B*, **26**, 4199 (1982).
7. W. R. Wadt and P. J. Hay, *J. Chem. Phys.* **82**, 284 (1984).
8. R. A. Friesner, *Chem. Phys. Lett.* **116**, 39 (1985).
9. R. A. Friesner, *J. Chem. Phys.* **85**, 1462 (1986).
10. T. J. Martinez, Ph.D. thesis, UCLA, 1994.
11. C. C. Tazartes, Ph.D. thesis, UCLA, 1997.
12. S. L. Marple, Jr., *Digital Spectral Analysis with Applications*, Prentice–Hall, Englewood Cliffs, NJ, 1987.
13. W. H. Press, S. A. Teukolsky, W. T. Vetterling, and B. P. Flannery, *Numerical Recipes in C*, Cambridge University Press, New York, 1992.
14. C. Lanczos, *Applied Analysis*, Dover, New York, 1988, p. 272.
15. G. Golub and C. Van Loan, *Matrix Computations*, Johns Hopkins University Press, Baltimore, MD, 1989.
16. T. J. Martinez and E. A. Carter, *J. Chem. Phys.* **100**, 3631 (1994).
17. M. N. Ringnalda, J. M. Langlois, B. H. Greeley, T. V. Russo, R. P. Muller, B. Marten, Y. Won, R. E. Donnelly, Jr., W. T. Pollard, G. H. Miller, W. A. Goddard III, and R. A. Friesner, *PS-GVB v1.00*, Schrödinger, Inc. New York, 1993.
18. T. J. Martinez and E. A. Carter, in *Modern Electronic Structure Theory Part II*, vol. 2, D. R. Yarkony, Ed., *Advanced Series in Physical Chemistry*, World Scientific, Singapore, 1995, p. 1132.
19. A. Sepehr, C. C. Tazartes, and E. A. Carter, unpublished results.
20. T. H. Dunning, Jr., *J. Chem. Phys.* **53**, 2823 (1970).
21. T. J. Martinez and E. A. Carter, *J. Chem. Phys.* **102**, 7564 (1995).